Applied Catalysis B: Environmental 147 (2014) 904–911

Contents lists available at ScienceDirect

Applied Catalysis B: Environmental

journal homepage: www.elsevier.com/locate/apcatb

Plasma-catalysis of low TCE concentration in air using $LaMnO_{3+\delta}$ as catalyst

M.T. Nguyen Dinh[a], J.-M. Giraudon[a,*], J.-F. Lamonier[a], A. Vandenbroucke[b], N. De Geyter[b], C. Leys[b], R. Morent[b]

[a] Université Lille 1, Unité de Catalyse et Chimie du Solide UMR CNRS 8181, Bât. C3, Cité Scientifique 59655 Villeneuve d' Ascq, France
[b] Ghent University, Faculty of Engineering, Department of Applied Physics, Research Unit Plasma Technology, Sint-Pietersnieuwstraat 41, 9000 Ghent, Belgium

ARTICLE INFO

Article history:
Received 27 March 2013
Received in revised form 12 June 2013
Accepted 1 July 2013
Available online 23 July 2013

Keywords:
Plasma-catalysis
$LaMnO_3$
Ozone
TCE
Glow discharge

ABSTRACT

The oxidative decomposition of trichloroethylene (TCE; 500–600 ppmv) was investigated in synthetic (dry air) and humid air (RH = 18%) with NTP (non thermal plasma) at atmospheric pressure, both in the absence and presence of lanthanum manganite catalyst at 150 °C. In the absence of catalyst, TCE removal is enhanced with humidity (RH = 18%) while O_3 production is decreased. However, whatever the carrier gas the carbon mass balances are poor amounting to 25–30% due to the presence of polychlorinated by-products such as phosgene, dichloroacetyl chloride (DCAC) and trichloroacetaldehyde (TCAD). In the presence of catalyst, the TCE conversion significantly increased as compared to that of the plasma alone system. The perovskite catalyst can dissociate the in plasma produced ozone to oxygen radicals that decompose TCE. In dry air, the carbon mass balance keep rather poor (35% – 460 J/L) due to the structural transformation of the catalyst with chlorine. In dry air, an optimum temperature of the catalytic reactor is found to be 100 °C resulting from a compromise between catalyst deactivation and enhancement of the catalytic reactions. However, water remarkably promotes the carbon mass balance (75% – 460 J/L) due to the beneficial role of water which acts as a chlorine scavenger at the surface of the catalyst, therefore retarding the perovskite degradation.

1. Introduction

Volatile organic compounds (VOCs) are common air pollutants that have adverse effects on environment and human health. Increasing environmental awareness has motivated research into alternative methods to remediate VOC-contaminated air streams. In particular, among the various technologies of VOC removal non thermal plasmas (NTP) have been recognized to be relevant to remove such toxins from atmospheric pressure gas streams [1,2]. NTP are attractive in this regard due to their high efficiency for producing radicals and oxidizing agents to decompose the VOC molecule. Additionally, NTP generated in electrical discharges are able to use air over a wide range of gas flow rates and VOC concentrations.

However, the variety of reactive species formed in a NTP (OH and O radicals, other atomic species, ions and activated molecules) results in a wide spectrum of reaction pathways and products. Unfortunately, based on a large number of experimental results it has to be concluded that non-thermal plasma does not usually allow the simultaneous achievement of both a high conversion and a satisfactory selectivity with respect to the desired reactions.

However, their applications are greatly restricted by low energy efficiency and CO_2 selectivity as well as undesirable products (such as ozone). An attempt to overcome these limitations is to combine NTP with catalysis.

This novel technique applied to VOCs removal, which has been recently reviewed, combines the advantage of high selectivity from catalysis and the fast ignition/response from plasma technique [3–7]. Various types of discharge treatments with the catalyst being exposed to the active plasma volume (In Plasma Catalysis IPC) [8–14] or followed by low temperature catalytic combustion catalysts (Post Plasma Catalysis PPC) [15–18] have been investigated for the oxidation of chlorinated hydrocarbons such as trichloroethylene. A recent review has discussed the different plasma-catalysis processes encountered for TCE removal [5]. The TCE removal efficiency and destruction pathways mainly depend on the nature of background gas, type of discharge, location and nature of the catalyst. In PPC configuration, the catalysts already used are transition metal oxides such as MnO_2 [15–17] or noble metals such as gold mesoporous silica Au/SBA-15 [18], Pd(0.05 wt%)/Al_2O_3 [19]. The most efficient catalysts have shown to easily decompose ozone into reactive oxygen species to promote VOC total oxidation [17].

* Corresponding author. Tel.: +33 320436856.
E-mail address: jean-marc.giraudon@univ-lille1.fr (J.-M. Giraudon).

0926-3373/$ – see front matter © 2013 Elsevier B.V. All rights reserved.
http://dx.doi.org/10.1016/j.apcatb.2013.07.008

Furthermore, reports on plasma-catalysis mainly focused on the increase of the removal and energy efficiency of pollutants. Few studies have been conducted on the identification and reduction of the by-products, which may cause additional environmental pollution.

Among the various electrical discharges investigated in the literature, we here focus on a DC-excited glow discharge at atmospheric pressure in a multi-pin-to-plate electrode configuration [20–22]. Such DC non-thermal plasmas require a relative low installation cost compared to pulsed corona systems. Additionally, they are easy to scale up and can work at high flow rates [23,24]. Among the transition-metal catalysts, manganese oxides are well recognized as (i) efficient catalysts for Cl-VOC total catalytic oxidation [25–27] and (ii) active catalysts for O_3 decomposition[28–30]. Hence, $LaMnO_{3+\delta}$, which is an environment-friendly and inexpensive material, has been used as catalyst. In this work, we reported on the performance of PPC compared to NTP alone for the destruction of TCE in dry air and air contaminated with water (Relative Humidity RH = 18%) and carbon dioxide (≈500 ppmv).

2. Experimental part

2.1. Experimental set-up

The experimental set-up was described in Fig. 1. It consisted of reaction gas supply, a multi-pin-to-plate plasma chemical reactor (30 kV/20 mA negative DC power supply), a post plasma catalytic reactor and analytical instrumentation. Total oxidation of trichloroethylene (TCE) was carried out in synthetic air or air supplied by a compressor (RH 18%; CO_2 in the range 460–480 ppmv). Gaseous TCE-contaminated air was produced by passing air through pure liquid TCE kept in a water bath at fixed temperature. Further dilution in air was achieved in order to get a TCE concentration in the range of 500–600 ppmv. The total gas-flow rate in all experiments was 120 L/h.

The multi-pin-to-plate plasma source was based on the concept of a negative DC glow discharge [20,22]. A detailed description of the geometry of the plasma reactor and electrical measurements has been published elsewhere [31]. The electron density and energy of the discharge are approximately 108-109 cm^{-3} and 2-3 eV, respectively [22].

The post-plasma reactor was cylindrical and connected to the NTP reactor in series. This reactor was made in Pyrex glass, with an inner diameter of 2.0 cm and an effective length of 10.0 cm.

2.2. Experimental procedure

2.2.1. NTP experiments

The NTP experiments were conducted with a residence time in the NTP reactor of 2.16 s. The energy density (ED) was allowed to vary with time.

2.2.2. PPC experiments

The $LaMnO_{3+\delta}$ catalyst (0.5 g) diluted with carborundum (100 microns) in a ratio of 6:1 (wt) in order to avoid flow dynamic problems (contact time ≈0.1 s) was deposited in the catalytic reactor. The catalyst was pre-calcined at 350 °C for 4 h (1 °C/min) and cooled down to room temperature (RT) before being maintained at the temperature of the experiment. The experiments are denoted NTPX where X stands for the relative humidity.

2.2.3. Effect of humidity

TCE was stabilized in synthetic air (PPC-LM0-150) or air supplied by a compressor (PPC-LM18-150) for one night at RT. The reactive gaseous effluent was admitted on the catalyst for 1–2 h duration in order to get a constant TCE concentration at the outlet, meaning that initial adsorption–desorption equilibrium of TCE over the catalyst surface was achieved. Then the catalyst temperature was raised to 150 °C (1 °C/min) and maintained for one hour. NTP reactor was switched on and the energy density was then allowed to vary.

The experiments are denoted PPC-LMX-Y where LM stands for the Lanthanum Manganite catalyst, X the relative humidity and Y the temperature of the catalyst.

2.2.4. Effect of temperature

TCE was stabilized in synthetic air (PPC-LM0-RT) for one night while the catalyst was cooled down to RT after calcination. Then the same experimental procedure as above was adopted, except catalyst temperature was kept at RT. After plasma-catalysis treatment at RT, the stabilized TCE/air gaseous mixture was exposed to the catalyst non re-calcinated in a similar manner except final catalyst temperature of 100 °C. NTP reactor was switched on and the energy density output was then allowed to vary (PPC-LM0-100).

The TCE removal efficiency, C mass balance and Energy Density were defined as followed:

$$TCE\ removal\ efficiency: TRE(\%) = \left(1 - \frac{[TCE]_{out}}{[TCE]_{in}}\right) \times 100 \quad (1)$$

$$C\ mass\ balance\ (\%) = \frac{[CO_x]}{(2 \times ([TCE]_0 - [TCE])} \times 100 \text{ where } [CO_x] = [CO] + [CO_2] \quad (2)$$

$$Energy\ Density: ED(J/L) = \frac{W(J/s)}{Q(L/s)} \quad (3)$$

where W means the discharge power and Q the flow rate.

By-products were qualitatively analyzed by mass spectrometry (Omnistar GSD 301 O_2 Pfeiffer Vacuum) using Scan Bargraph mode (SEM voltage: 1600 V; acquisition rate: 1.5 scan/min; resolution: 50 electron ionization energy: 70 V) taking into account the procedure given in [31]. For by-product distribution $I_x/(I_{95\text{-}0} - I_{95})$ MS ratio in function of ED in NTP were given. I_x was the intensity of a representative fragment $m/z = x$ of the molecule under concern corrected from interfering species and $I_{95\text{-}0}$ was the initial intensity of the representative fragment of TCE ($m/z = 95$). This ratio allowed us to have an idea of the relative evolution of the selectivity of the organic by-products with energy density. The selected $x = m/z$ for the $I_x/(I_{95\text{-}0} - I_{95})$ estimation were 63, 82 and 83 for phosgene, TCAD and DCAC, respectively. FT-IR spectroscopy (Bruker, Vertex 70) was also used for the analysis of CO, CO_2, N_2O, HCl and other by-products with a long-path gas cell (optical length: 0.80 m; resolution: 4 cm^{-1}). After calibration of the FT-IR instrument for CO and CO_2, a peak area in IR absorbance was adopted to calculate the concentration with a special care in CO peaks due to overlapping with ozone peak and N_2O peak. For experiments carried out with air from the compressor the atmospheric CO_2 contribution was removed to determine the actual CO_2 concentration. Ozone formation was analyzed by an ozone monitor (Envitec, model 450). Humidity measurements were performed using a Testo 445 measuring instrument.

2.3. Catalyst preparation and characterization

$LaMnO_{3+\delta}$ was synthesized via the amorphous citrate precursor method. Stoichiometric amounts of aqueous solution of the salts of the corresponding metal nitrates ($La(NO_3)_3.6H_2O \geq 99.0\%$ Fluka, $Mn(NO_3)_2.6H_2O$ Aldrich, $C_6H_8O_7$ Fluka) were mixed with an aqueous solution of citric acid so that the ratio of the number of total metal moles to that of citric acid was equal to one. The resulting

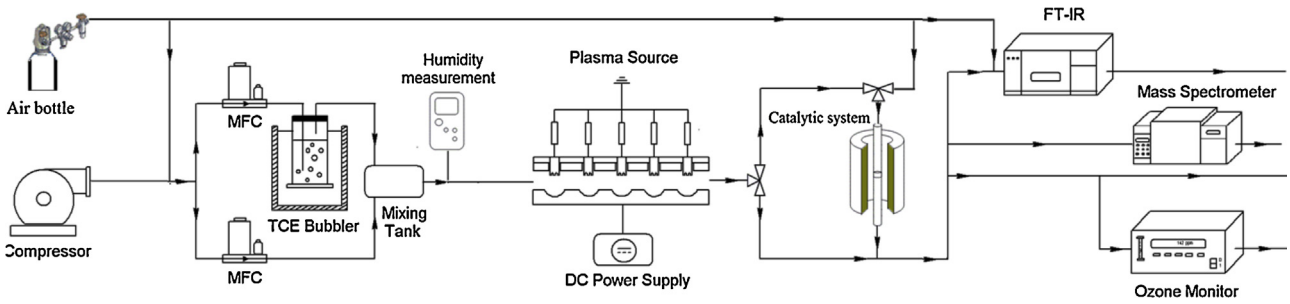

Fig. 1. Experimental plasma-catalysis set-up.

solution was stirred at room temperature and evaporated at 60 °C for 2 h to obtain syrup. After drying in an oven at 100 °C overnight and then at 220 °C for 2 h the resulting powder was calcined in air at 700 °C (2 °C/min) for 10 h.

Phase analysis was performed by X-ray powder diffraction using a D8 Advance-Brücker using the $K_{Cu\alpha 1}$ = 1.54056 Å. The specific surface areas were measured with a sorptometer Quantasorb Junior using the single point BET surface area determination. Prior to measurement, the catalysts were subjected to a final purging while they were heated to 150 °C in flowing N_2 for 1 h.

XPS spectra of the catalysts were recorded using a Kratos AXIS Ultra DLD spectrometer with a monochromatic Al Kα radiation source ($h\nu$ = 1486.7 eV) operating at 15 kV and 10 mA. High resolution (0.1 eV) spectra were then recorded for pertinent photoelectron peaks at pass energy of 40 eV to identify the chemical state of each element. All the binding energies (BEs) were referenced to the C1s neutral carbon peak at 285 eV. The processing and curve-fitting of the high resolution spectra was performed using CasaXPS™ software.

3. Results and discussion

3.1. Destruction of TCE with NTP

Fig. 2 shows the TCE conversion, the CO_x and O_3 concentrations in function of ED in NTP0 and NTP18 experiments. Compared to NTP0, TCE conversion linearly increases with ED but more rapidly in the presence of water with a slope ratio S_{18}/S_0 of about 1.3. At 500 J/L (16.7 W) the TCE conversion of 73% (NTP0) increases to 85% for NTP18. Therefore, adding small amounts of water appears to be more advantageous from the point of view of TCE decomposition. This might be related to the increase of hydroxyl radicals which may be formed from water. These radicals are well known to be stronger oxidants than others such as oxygen atoms and peroxyl radicals. However, irrespective of the experiments, the carbon mass balance is rather low, about 30% at 500 J/L, with CO as predominant form. The ozone production increases with energy input to achieve a level of 180 and 280 ppm at 460 J/L in wet and dry mixtures, respectively. Hence, O_3 production reduces by one third with water indicating the adverse effect of low humidity on ozone formation.

3.2. Destruction of TCE with PPC

It must be mentioned that the XRD pattern of the fresh lanthanum manganite sample (not shown here) exhibits only the rhombohedral phase of $LaMnO_{3+\delta}$ having a specific surface area of 15 m^2/g. Fig. 3a and b show the TCE conversion, the amount of CO_x produced in function of SED in PPC-LM0-150 and PPC-LM18-150 experiments. When adding water, a significant increase of the TCE conversion for ED less than 460 J/L is observed whereas the discrepancies reduce after that, with TRE reaching 88 and 93% for dry and humid air, respectively. It is remarkable that the carbon mass balance is significantly improved when adding water vapor, 75% (RH18) compared to 35% (RH0) while the molar CO_2/CO ratio is poorly affected (0.7 and 0.6).

Fig. 3c and d are related to the performances of the NTP activated catalyst regarding the NTP treated effluent. At 460 J/L the conversion of the remaining TCE amounts to about 65%. For PPC-LM18-150, a linear evolution is observed between TCE conversion, CO_x production and O_3 consumption for ED ≤ 300 J/L. This shows that O_3 catalytic decomposition produces active oxygen species that are able to convert part of the remaining TCE. Regarding the formal equation below:

$$C_2Cl_3H + 4O_3 \rightarrow 2CO_2 + Cl_2 + HCl + 4O_2$$

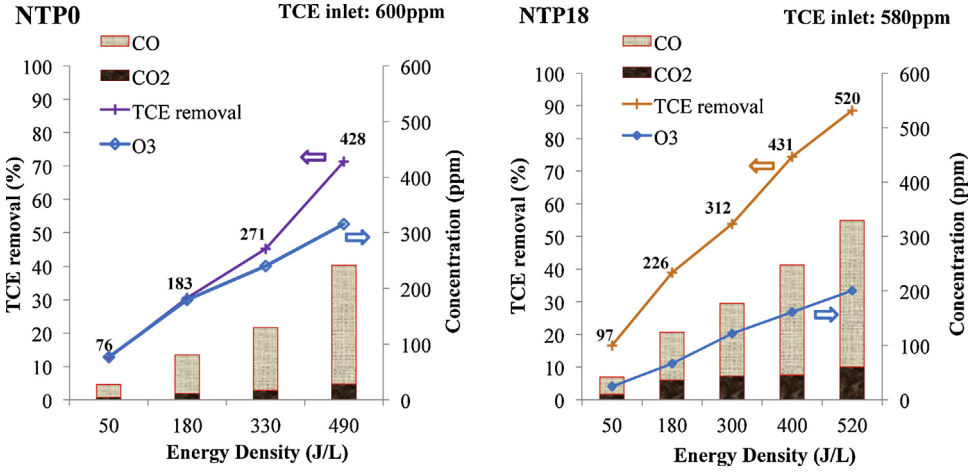

Fig. 2. TRE, CO_x and O_3 concentrations in function of ED in NTP0 and NTP18 experiments (in bolt converted TCE in ppmv).

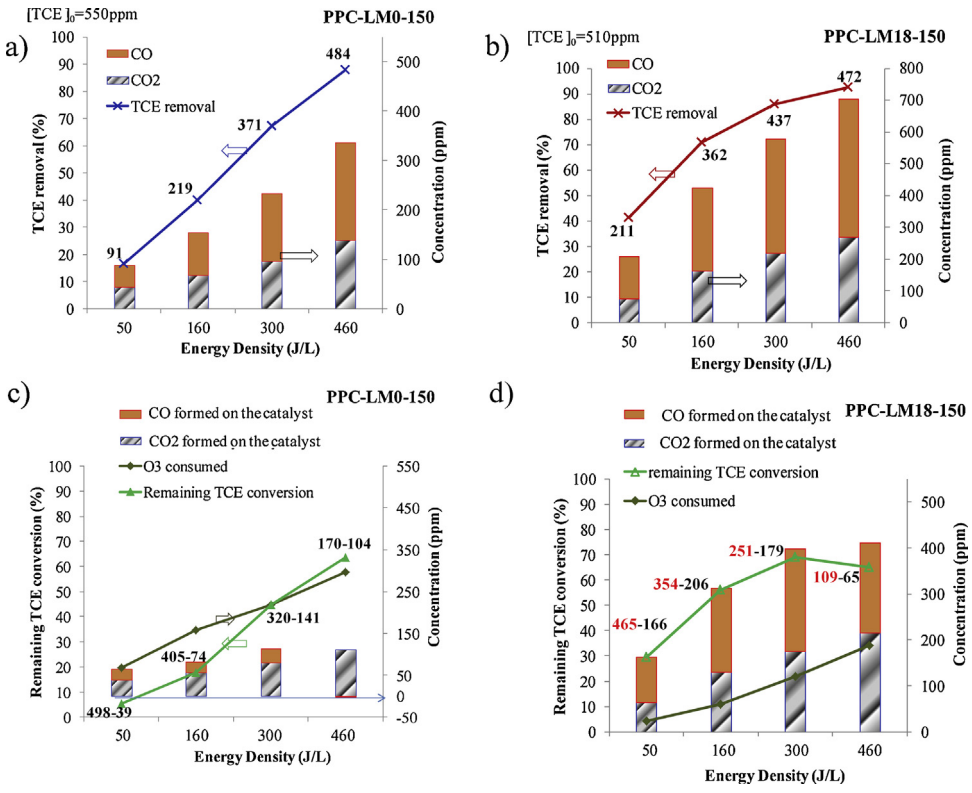

Fig. 3. TRE, CO_x productions in function of ED in a) PPC-LM0-150 and b) PPC-LM18-150 experiments (in bolt: converted TCE in ppmv). Remaining TRE, CO_x production and O_3 consumption in function of ED in c) PPC-LM0-150 and d) PPC-LM18-150 experiments (in bolt remaining TCE-converted remaining TCE in ppmv).

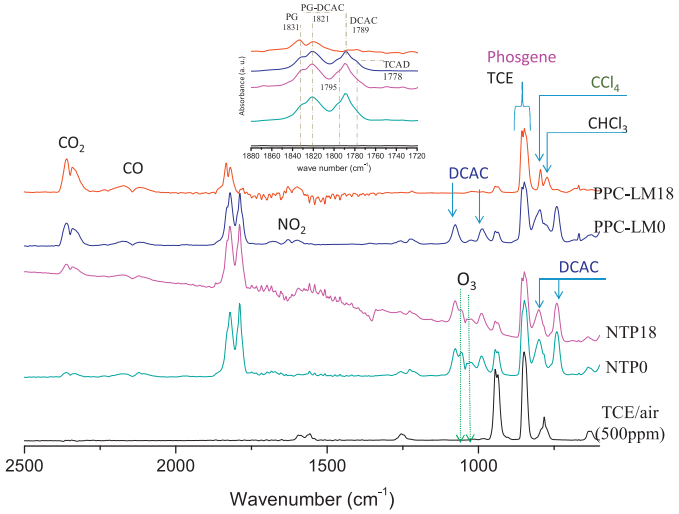

Fig. 4. FT-IR spectra between 850 and 2500 cm^{-1} of TCE at the inlet and after the plasma and PPC experiments.

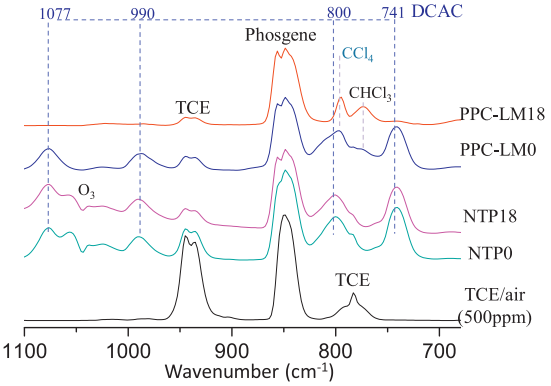

Fig. 5. FT-IR spectra between 680 and 1100 cm^{-1} of TCE at the inlet and after the plasma and PPC experiments.

The molar ($O_{3consumed}/TCE_{reacted}$) ratio being less than 4 at low ED implies that other degradation schemes must be considered. At 460 J/L the molar ($CO_x/TCE_{reacted}$) ratio of about 8 clearly shows that the increase of energy enhances the capacity of the catalyst to efficiently destroy the polychlorinated by-products generated in the plasma into CO_x (see below). However, in dry air the plasma-assisted catalyst appears only as active as in humid air at the highest ED. The catalyst is poorly selective in CO_2 suggesting modifications of the catalyst.

3.3. Reaction by-products of TCE decomposition

Figs. 4 and 5 show the FT-IR spectra of both the inlet and outlet stream when the plasma is operated in the same conditions in NTP and PPC experiments, respectively. In NTP, whatever the nature of the carrier gas, along with CO_x formation some polychlorinated by-products have already been partly detected by FT-IR and MS [31]. These include phosgene [32–34], DCAC [35] and TCAD [36–37]. Another n(C=O) vibration band arising at 1395 cm^{-1} can also been observed. Its attribution is at the moment questionable. A previous work reported a value of 1794 cm^{-1} for that band in formylchloride (ClCHO, 1795 cm^{-1}) [38], but in another study the observance of that band is at 1984 cm^{-1} [39]. Chlorine is also eliminated as HCl (not seen in the figure) and Cl_2 (MS). Formation of ozone and traces of N_2O are also detected in the outlet stream. In plasma alone, collisions of accelerated electrons or radicals with

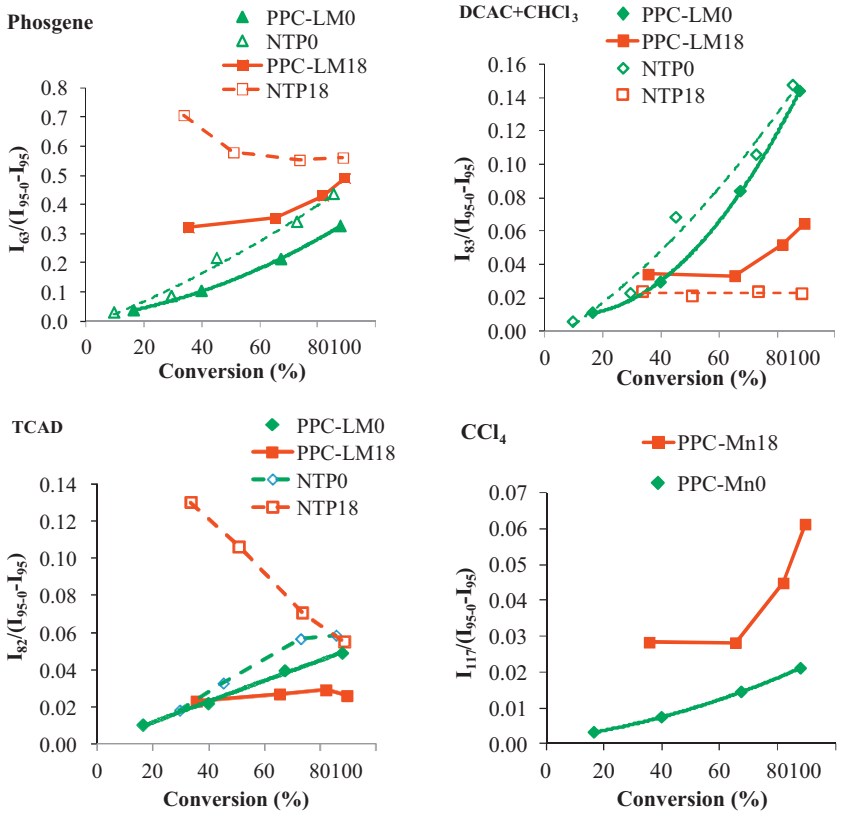

Fig. 6. Evolution of $I_x/(I_{95\text{-}0} - I_{95})$ in function of TCE conversion in NTP and PPC experiments.

VOC with molecules from the carrier gas (N_2 and O_2) induce reactions of dissociation. In dry air O_2^*, N_2^* or electrons can react with TCE to give TCE° and Cl°. Cl° can easily react with the reactive double bond of the TCE to give either $(CCl_3)CHCl°$ or $(CHCl_2)CCl_2°$. $(CCl_3)CHCl°$ and $(CHCl_2)CCl_2°$ after reaction with oxygen species (O) and Cl° departure give $(CCl_3)CHO$ (trichloroacetaldehyde) and $(CHCl_2)COCl$ (dichloroacetylchloride) respectively. C-C bond cleavage and Cl° attack can lead to the formation of phosgene, CO, CO_2, Cl_2, HCl [17].

In the presence of humidity direct dissociation of water allows giving the efficient OH°. These species can react with the carbon-carbon double bond of TCE to give CHCl(OH)-$CCl_2°$. After reaction with O_2 the resulted peroxyl radicals transform after radical coupling into chloroethoxyl radicals which can decompose to give phosgene [40]. This pathway can account for the high production of phosgene in NTP0 experiment.

When the plasma processed gases, including non-decomposed TCE, ozone and other by-products, were passed through $LaMnO_{3+\delta}$ catalyst introduced downstream of the plasma reactor, the FT-IR spectra show a decrease in TCE concentration, the disappearance of O_3 as well as the increase of CO_x production (Figs. 4 and 5). Furthermore, DCAC was largely decomposed by passing through the catalyst in humid air. However, DCAC did not decompose in dry air. In addition phosgene and TCAD were decreased, to a lesser extent, when passing through $LaMnO_{3+\delta}$ catalyst. Although Cl_2CO is a toxic industrial chemical, it can be easily removed from the gas stream by simple post-treating with a caustic scrubber. In addition, the appearance of new bands at 794 and 773 cm^{-1} ascribed to C-Cl vibration reveals the presence of two new chlorinated C1 species (Fig. 5), namely tetrachloromethane (CCl_4) and chloroform ($CHCl_3$), respectively.

Fig. 6 shows the relevant $I_x/(I_{95\text{-}0} - I_{95})$ ratios (see experimental part) in function of the TCE conversion for the different experiments. As expected, these ratios are always lower in PPC experiments compared to NTP ones whatever the TCE conversion under concern, indicating the beneficial role of the catalyst. For NTP it is remarkable that the relative phosgene production is enhanced compared to those of DCAC and TCAD with humidity. Increasing the TCE conversion in humid air allows to keep the $I_{83}/(I_{95\text{-}0} - I_{95})$ ratio stable while decreasing the $I_{82}/(I_{95\text{-}0} - I_{95})$ and $I_{63}/(I_{95\text{-}0} - I_{95})$ ratios, respectively. Hence, DCAC and TCAD species having a simple carbon–carbon bond were easily broken in the subsequent catalytic reaction into CO_x, HCl, Cl_2 and Cl_2CO (for DCAC) as well as to a minor extent to $CHCl_3$ and CCl_4 with water vapor. In dry air, DCAC is poorly decomposed suggesting catalyst restructuration. Along N_2O traces of NO_2 have also been detected. The production of Cl_2 and HCl have been monitored by mass-spectroscopy. The $(I_{36}/I_{95\text{-}0} - I_{95})$ and $(I_{70}/I_{95\text{-}0} - I_{95})$ MS ratios which reflect the selectivity of HCl and Cl_2 respectively have been plotted in function of ED in the course of the PPC experiments in dry and wet air (Fig. 7). As shown in the figure the production of HCl and Cl_2 increase with TCE conversion.

In the presence of oxygen without water, the amount of Cl_2 is significantly increased compared to the conditions with humidity. Cl_2 can be a priori be formed from the Deacon reaction over possible MnO_xCl_y species which are recognized as possible catalyst of the Deacon reaction but, as already mention, the temperatures (£150 °C) are very low for the reaction to occur at a significant rate. However chlorine can also be removed from the surface in accordance with the following reaction:

$$LaMnO_{(3+d-(x/2))}Cl_x + x/4O_2 = LaMnO_{3+d} + x/2Cl_2.$$

The additional of water can limit the formation of Cl_2 through the Deacon reaction but the effect must be minor due to the low operating temperature. We believe that water plays a role in the removal of surface chlorine forming thus hydrogen chloride. The decrease of the Cl_2 production can be explained by the change in

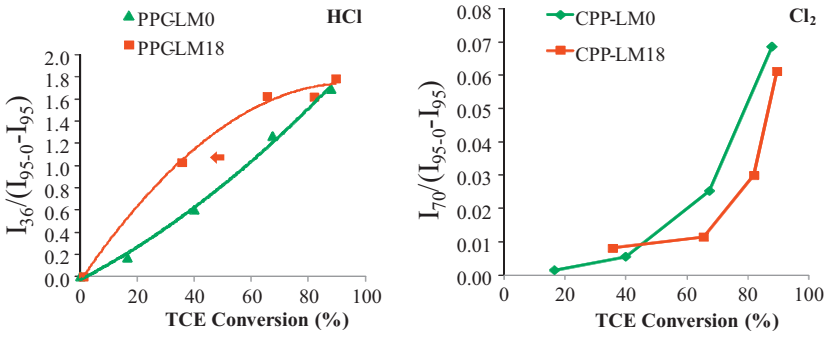

Fig. 7. Evolution of $I_x/(I_{95\text{-}0} - I_{95})$ ($x = 36$, HCl; $x = 70$; Cl_2) in function of TCE conversion in PPC experiments.

the mechanism of regeneration of the perovskite as already proposed in the literature [27,41] in agreement with the following reactions:

$$LaMnO_{(3+d-(x/2))}Cl_x + xH_2O = LaMnO_{(3+d-(x/2))}(OH)_x + xHCl.$$

$$LaMnO_{(3+d-(x/2))}(OH)_x = LaMnO_{3+d} + xH_2O.$$

Also organic Cl adsorbed species decrease with humidity. It is believed that the chlorine based organic species are destroyed more easily due to the fact that the amount of active sites is higher in wet air due to efficient regeneration of the active sites of the reactions.

3.4. Effect of the temperature

Fig. 8 shows the conversion of TCE and the carbon mass balance in function of ED for different operating temperatures of the catalyst in dry air. It must be reminded that the experiment at 100 °C is carried out just after the one performed at RT on contrary to the two other ones which have been performed on fresh catalysts. It is noticeable that, whatever the temperature under concern, adding

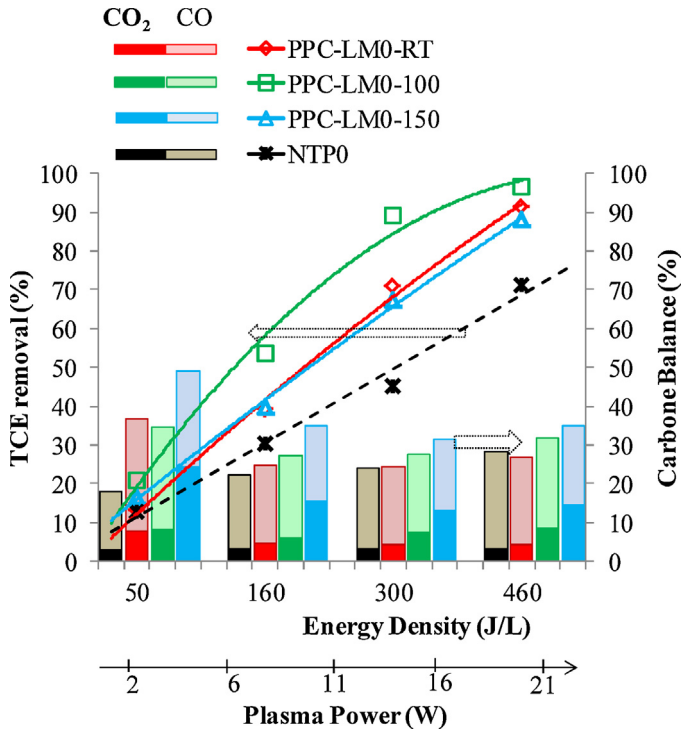

Fig. 8. Effect of the temperature on the TCE conversion and the carbon mass balance in function of ED.

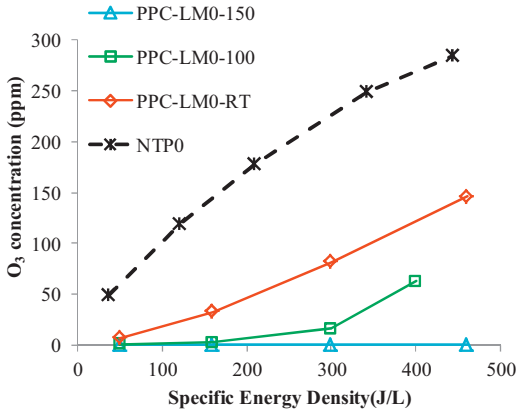

Fig. 9. O_3 concentration at the exit of the post-plasma catalytic reactor.

a catalyst downstream the plasma reactor speeds up the reaction. At 460 J/L, the activity ranks as follows: PPC-LM0-100 (97) > PPC-LM0-RT (91) ≈ PPC-LM0-150 (88). Carbon mass balances as well as CO_2 productions slightly increase with temperature. It is expected that the increase of the temperature of the catalyst reactor may increase the thermal decomposition of ozone in the vicinity of the catalyst leading to a decrease of the disposal of O_3 to be catalytically decomposed on the catalyst. At the same time reactions at the catalyst surface, such as decomposition of ozone and interactions between reactive adsorbed oxygen atoms and TCE and related gaseous polychlorinated by-products, are also accelerated. Fig. 9 shows the uptake of O_3 at different temperatures compared to the amount of ozone detected at the exit of the NTP in function of ED. Ease of catalytic ozone decomposition increases with temperature even though 10% of O_3 has been estimated to be thermally destroyed at 150 °C.

Hence the improvement of TRE when adding a catalyst is related to its ability to dissociate ozone. Nevertheless, it is surprising that the optimum temperature for TRE is at 100 °C. A compromise between catalyst deactivation and enhancement of the catalytic reactions may account for such an observation. Regarding the by-products distribution, its nature does not change with temperature. However, it is noticeable that CCl_4 and $CHCl_3$ relative amounts increase with temperature.

3.5. XPS characterization of the used catalysts

Table 1 presents the atomic composition at the surface of the samples before and after PPC in synthetic air (LM-sa) and ambient air (LM-aa). The XPS atomic La/Mn ratio of the fresh catalyst of 1.61 shows lanthanum enrichment at the surface of the catalyst in accordance with the well-known affinity of La^{3+} to react with humidity and CO_2 of ambient air. This ratio remains stable

Table 1
XPS results of the fresh and tested catalysts.

Samples	Experiments	XPS composition	
		Before test	After test
LM-sa	PPC-LM0-150	$LaMn_{0.62}O_{3.46}C_{1.84}$	$LaMn_{0.49}O_{7.64}C_{5.15}Cl_{1.42}$
LM-aa	PPC-LM18-150		$LaMn_{0.61}O_{4.21}C_{2.16}Cl_{0.87}$

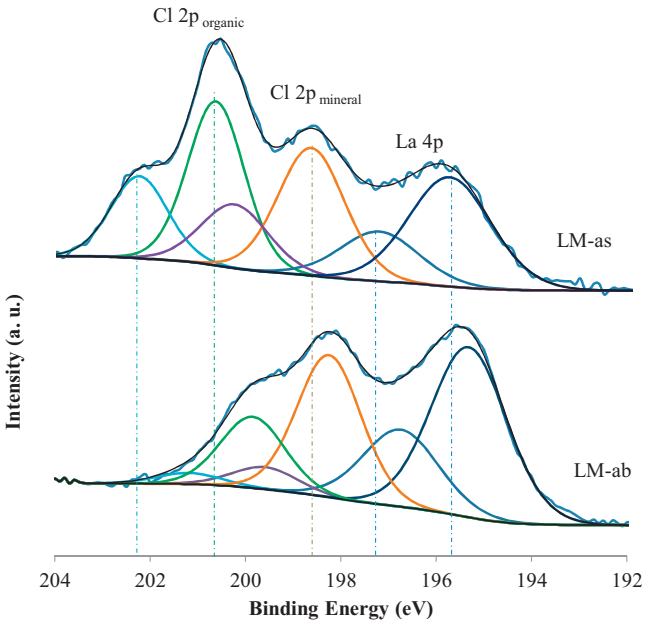

Fig. 10. XPS of the La 4p and Cl 2p envelop of the tested catalysts.

after conducting the test in humid air and significantly increases in dry air. One also notices important carbon enrichment on LM-sa. The high carbon content is explained by the presence of a C1s peak at 282.7 eV ascribed to SiC used as catalyst diluent. High concentrations of chlorine are detected by XPS: 1 Cl atom per 1 M atom (M = La, Mn) to 2 M atoms with humid and dry air, respectively, for an exposure duration to the reactive gaseous effluent of 6 h. Hence, in dry air the extent of chlorine deposit is greatly enhanced compared to humid conditions. Fig. 10 shows the decomposition of the Cl 2p and La 4p signals for the tested catalysts. Each envelop can be decomposed into 6 photo-peaks. The two photo-peaks at the lowest binding energies (B.E.) are characteristic of the spin-orbit components La $4p_{3/2}$ and La $4p_{1/2}$. The other four characterize the Cl $2p_{3/2}$ and Cl $2p_{1/2}$ components of two distinct chlorine phases (c.f. Table 1). The B.E. of the Cl $2p_{3/2}$ component at 198.3 and 198.7 eV clearly identify mineral chlorine [42]. Formation of (oxi)chlorinated manganese species and oxichlorinated lanthanum could be expected. The value observed at 198.3 eV on LM-aa is lower than the one observed on $MnCl_2$ (199.2 eV) but matches perfectly to the binding energy of LaOCl Cl $2p_{3/2}$ at 198.3 eV [26]. This indicates that chlorine atoms are preferentially linked to lanthanum.

The second Cl $2p_{3/2}$ component at 200.3 ± 0.4 eV is ascribed to (oxi)chlorinated organic species such as $CH_xCl_y(O_z)$. A lowering of the $(Cl_{org}/Cl_{min})_{XPS}$ atomic ratio is shown in humid air (Fig. 10). These results highlight the role of water which is able to partly clean up the catalyst surface from chlorine and to delay the perovskite degradation with time on stream.

4. Conclusion

The decomposition of trichloroethylene was investigated by NTP generated in a DC-excited atmospheric pressure glow discharge using a multi-pin-to-plate electrode configuration and post-plasma catalysis using $LaMnO_{3+\delta}$ as catalyst. The carrier gas was dry synthetic air and humid air (RH: 18%). Regarding the NTP process alone:

- The TCE removal efficiency is enhanced in humid air due to the strong oxidation power of OH radicals.
- The carbon mass balances are poor (25–30%) and polychlorinated by-products such as phosgene, DCAC and TCAD are observed along with CO_x, Cl_2 and HCl.
- The O_3 production decreases with humidity.

Regarding the PPC experiments:

- Adding a catalyst downstream the NTP reactor enhances the performances of the process in humid air in terms of TCE removal efficiency and CO_2 selectivity due to the ability of the catalyst to decompose O_3 to generate active oxygen species able to oxidize part of the unreacted TCE and of the polychlorinated by-products.
- The TCE removal efficiency shows an optimal temperature at 100 °C in dry air.
- The influence of water is remarkable. Despite the fact that water is able to block the active sites, the performances for TCE degradation are enhanced in humid air due to the role of water to act as a chlorine scavenger at the surface of the catalyst.

Hence, the combination of a DC glow discharge plasma with lanthanum perovskite as post plasma catalyst increases the overall performances of the process compared to those of the NTP alone for TCE abatement in humid air.

Acknowledgement

The authors would like to thank the PHC Tournesol FL (No. 25462PJ) and the Nord Pas de Calais region–CNRS. R. Morent acknowledges the support of the Research Foundation Flanders (FWO) for a post-doctoral research fellowship.

References

[1] K. Urashima, J.-S. Chang, IEEE Trans. Diel. Electr. Insul. 7 (5) (2000) 602.
[2] H.H. Kim, Plasma Process Polym. 1 (2) (2004) 91.
[3] J. Van Durme, J. Dewulf, C. Leys, H. Van Langenhove, Appl. Catal. B: Environ. 78 (3–4) (2008) 324.
[4] H.L. Chen, H.M. Lee, S.H. Chen, M.B. Chang, S.J. Yu, S.N. Li, Environ. Sci. Technol. 43 (2009) 2216.
[5] A.M. Vandenbroucke, R. Morent, N. De Geyter, C. Leys, J. Hazard. Mater. 195 (2011) 30–54.
[6] A.M. Vandenbroucke, R. Morent, N. De Geyter, C. Leys, J. Adv. Oxid. Technol. 14 (2011) 165.
[7] A.M. Vandenbroucke, R. Morent, N. De Geyter, C. Leys, J. Adv. Oxid. Technol. 15 (2012) 232.
[8] T. Oda, T. Takahashi, S. Kohzuma, IEEE Trans. Ind. Appl. 37 (4) (2001) 965.
[9] T. Oda, T. Takahahshi, K. Yamaji, IEEE Trans. Ind. Appl. 38 (3) (2002) 873.
[10] T. Oda, T. Takahahshi, K. Yamaji, IEEE Trans. Ind. Appl. 35 (2) (2002) 373.
[11] T. Oda, K. Yamaji, T. Takahashi, IEEE Trans. Ind. Appl. 40 (2) (2004) 430.
[12] R. Morent, J. Dewulf, N. Steenhaut, C. Leys, H. Van Langenhove, J. Adv. Oxid. Technol. 9 (1) (2006) 53.
[13] M. Magureanu, N.B. Mandache, V.I. Parvulescu, C. Subrahmanyam, A. Renken, L. Kiwi-Minsker, Appl. Catal. B: Environ. 74 (3–4) (2007) 270.
[14] C. Subrahmanyam, A. Renken, L. Kiwi-Minsker, Chem. Eng. J 134 (1–3) (2007) 78.
[15] T. Oda, K. Yamaji, T. Takahashi, IEEE Trans. Conf. Rec. 2002, vol. 1–4, IEEE Ind. Appl. Conf., 2002, p. 1822.
[16] S.B. Han, T. Oda, R. Ono, IEEE Trans. Ind. Appl. 41 (5) (2005) 1343.
[17] S.B. Han, T. Oda, Plasma Sources Sci. Technol. 16 (2) (2007) 413.
[18] M. Magureanu, N.B. Mandache, J.C. Hu, R. Richards, M. Florea, V.I. Parvulescu, Appl. Catal. B: Environ. 76 (3–4) (2007) 275.
[19] A.M. Vandenbroucke, R. Morent, N. De Geyter, M.T. Nguyen Dinh, J.-M. Giraudon, J.-F. Lamonier, C. Leys, Int. J. Plasma Environ. Sci. Technol. 4 (2–9) (2010) 135.
[20] Y.S. Akishev, A.A. Deryugin, I.V. Kochetov, A.P. Napartovich, N.I. Trushkin, J. Phys. D: Appl. Phys. 26 (1993) 1630.

[21] Y.S. Akishev, M. Grushin, I.V. Kochetov, A.P. Napartovich, M. Pan'kin, N.I. Trushkin, Plasma Phys. Rep. 26 (2000) 157.
[22] Y.S. Akishev, O. Goossens, T. Callebaut, C. Leys, A.P. Napartovich, N.I. Trushkin, J. Phys. D: Appl. Phys. 34 (2001) 2875.
[23] R. Vertriest, R. Morent, J. Dewulf, C. Leys, H. Van Langenhove, Plasma Sources Sci. Technol. 12 (3) (2003) 412.
[24] R. Morent, C. Leys, Ozone Sci. Eng. 27 (3) (2005) 239.
[25] G. Sinquin, J.P. Hindermann, C. Petit, A. Kiennemann, Catal. Today 54 (1999) 107.
[26] G. Sinquin, C. Petit, J.P. Hindermann, A. Kiennemann, Catal. Today 70 (2001) 183.
[27] G. Sinquin, C. Petit, S. Libs, J.P. Hindermann, A. Kiennemann, Appl. Catal. B: Environ. 32 (2001) 37.
[28] W. Li, G.V. Gibbs, S.T. Oyama, J. Am. Chem. Soc. 120 (1998) 9041.
[29] W. Li, S.T. Oyama, J. Am. Chem. Soc. 120 (1998) 9047.
[30] R. Radhakrishnan, S.T. Oyama, J.G. Chen, K. Asakura, J. Phys. Chem. B 105 (2001) 4245.
[31] A.M. Vandenbroucke, M.T. Nguyen Dinh, J.-M. Giraudon, R. Morent, N. De Geyter, J.-F. Lamonier, C. Leys, Plasma Chem. Plasma Process. 31 (2011) 707.
[32] I. Hannus, I. Kiricsi, Gy. Tasi, P. Fejes, Appl. Catal. 66 (1990) L7.
[33] J. Fan, J.T. Yates, J. Am. Chem. Soc. 118 (1996) 4686–4692.
[34] S.-K. Joung, T. Amemiya, M. Murabayashi, R. Cai, K. Itoh, Surface Science 598 (2005) 174–184.
[35] A. Miyake, I. Nakagawa, T. Miyazawa, I. Ichishima, T. Shimanouchi, S. Mizushima, Spectrochimica Acta 13 (1958) 161.
[36] L.J. Bellamy, R.L. William, J. Chem. Soc. (1958) 3465–3468.
[37] G. Lucazeau et, A. Novak, Spectrochimica Acta 25A (1968) 1615–1629.
[38] J. Borisch, S. Pilkenton, M.L. Miller, D. Raftery, J.S. Francisco, J. Phys. Chem. B 108 (2004) 5640–5646.
[39] H. Niki, P.D. Maker, L.P. Breitenbach, C.M. Savage, Chem. Phys. Lett. 57 (1978) 4.
[40] R. Atkinson, Chemical Reviews 85 (1985) 69–201.
[41] D. Kiessling, R. Schneider, P. Kraak, M. Haftendorn, G. Wendt, Appl. Catal. B 19 (1998) 143.
[42] C.D. Wagner, W.M. Riggs, L.E. Davis, J.F. Mulder, in: G.E. Muilenberg (Ed.), Handbook of X-ray Photoelectron Spectroscopy, PerkinElmer Corporation, Eden Prairie, 1978.